

FULL-CYCLE STATE EVALUATION OF S700K SWITCH MACHINE BASED ON RESIDUAL NETWORK AND FUZZY CLUSTERING

WENJUN WEI¹, XUANMING ZHANG^{1,*} AND LIBEN YANG²

¹School of Automation and Electrical Engineering

²Key Laboratory of Opto-Technology and Intelligent Control, Ministry of Education

Lanzhou Jiaotong University

No. 88, Anning West Road, Anning District, Lanzhou 730070, P. R. China

weiwenjun@mail.lzjtu.cn; yangliben0880@163.com

*Corresponding author: zhangxm0213@163.com

Received November 2021; revised March 2022

ABSTRACT. *In normal, sub-health, fault, critical fault, and other full-cycle operating states of the S700K switch machine, the differences of state characteristics are slight and the fault data is small, making it difficult to diagnose the whole life cycle. Considering the consistency of its active power curve and state, this paper proposes a full-cycle operating state diagnosis algorithm for the S700K switch machine based on residual network and fuzzy clustering. The pre-trained ResNet residual network is selected, the classification layer is removed, and only the feature extraction layer is retained. Secondly, the S700K power curve image is input into the network, and the S700K feature data is extracted from the global pooling layer of the network after the residual convolution operation. Thirdly, the characteristic data of different running states are combined into an eigen-vector matrix. Then, the fuzzy similarity matrix is obtained by using the fuzzy clustering method. When the confidence factor λ changes from 0 to 1, a dynamic clustering diagram is formed to obtain the classification result of the full-cycle operating state. The experimental results show that even though it is not trained, the algorithm can be applied to diagnosing the S700K switch machine in the whole cycle state. In addition, through field data detection and verification, it can effectively identify the full-cycle operating state of the switch machine.*

Keywords: S700K switch machine, The whole cycle, Residual network, ResNet, Fuzzy cluster

1. Introduction. The S700K electric switch machine is essential outdoor signal equipment in China's high-speed railway transportation. Its primary function is to convert and lock the turnout and reflect the position and working state of the turnout. As outdoor equipment, the S700K switch machine is often affected by a series of external influences such as weather and external forces. Statistics show that the signal equipment failures of a railway bureau in the recent four years accounted for more than 40% of the total number of signal equipment failures [1]. Currently, the state diagnosis of the S700K switch machine in China is mainly caused by analysis and planned maintenance after failure. It relies on manual experience and regular investigation, detection, and maintenance. With the increase of high-speed rail lines and total mileage in China, this method can no longer meet the current stage of fault monitoring. Effective identification of the S700K switch machine's working state, namely normal, sub-health, fault, and serious fault, is significant to the operation safety of the high-speed railway. Significantly, finding sub-health state will significantly improve the maintenance efficiency and eliminate accidents in the embryonic

stage. At present, the state diagnosis of the whole cycle is less, mainly focusing on fault diagnosis. At present, the state diagnosis of the whole cycle is more petite, mainly focusing on fault diagnosis. The early fault diagnosis of the S700K switch machine mainly uses time domain, frequency domain, time-frequency domain, and other methods to decompose and extract features of curve signals. [1] uses PLSA to extract features and map fault features to the topic space. [2] uses EEMD to decompose the power curve to extract features and then uses fuzzy clustering for classification. In [3], the grey correlation degree between curves is calculated, and the fault is identified according to its size. The above methods deal with the fault curve, but the fault curve of the switch machine is quite different from the standard curve, and the extracted features are significantly different. However, because the difference between sub-health and health state is minimal, these methods are not suitable for full-cycle state diagnosis, and methods with more robust feature extraction must be introduced.

In recent years, deep learning has made significant progress in fault detection, which significantly improves fault detection accuracy by utilizing the feature extraction and classification capabilities of a convolutional neural network. [4] uses 1D-CNN to realize the integration of feature extraction and fault recognition. [5] uses deep learning to input the B-display image of rail damage into the ResNet residual network for classification and detection. [6] combines image processing with deep learning to detect motorized static contacts in a switch. [7] constructs a deep learning model to realize early fault diagnosis under time-varying conditions. A deep convolutional network has a robust feature extraction capability, but as the number of layers increases, the gradient will disappear, and it cannot be trained. As an improved model, deep learning residual network solves the gradient disappearance by introducing direct network connection at different layers [8-11]. The above method requires a large amount of data to train the model before fault detection. As an unsupervised classification method, fuzzy clustering can be classified without training by applying the principle of fuzzy mathematics and has been applied in different fields [12-14]. For this reason, this paper uses the advantages of the residual network to extract solid features and the feature of fuzzy clustering classification that does not require training and combines the two methods to propose a method for the complete cycle state diagnosis of the S700K switch machine.

1) Input the action power curve of the S700K switch machine into the pre-trained residual network ResNet-18 in the form of images.

2) The first 17 layers of the residual network, namely feature extraction, were used to remove the classification layer of the network, and 512 features were extracted from the global pooling layer after the convolutional residual operation.

3) Build a feature matrix from the extracted feature vectors, and use fuzzy clustering of feature vector matrices under different operating conditions to obtain a fuzzy similarity matrix. When the confidence factor changes from 0 to 1, a dynamic clustering graph is formed to obtain the complete cycle classification result of running status.

The rest of this paper is constructed as follows. In the second section, the characteristics of switch machine in various operating states are analyzed. The third section introduces residual network and feature extraction process of switch machine. In the fourth section, fuzzy clustering method is introduced. In the fifth section, switch machine evaluation process and corresponding experimental analysis are introduced. Finally, conclusions are drawn in the sixth section.

2. State Curve Analysis of S700K Switch Machine. The switch machine is an executive device that operates the switch to complete the conversion, and the S700K is an electric switch machine mainly used in China's high-speed railways. During the

traction conversion process of the switch, the translation movement of the action rod can be regarded as a single-axis drag movement. So the relationship between power and force F can be obtained as

$$F = \frac{30\Omega n_t}{\pi n v} P \quad (1)$$

In the formula, n_t , n , and v respectively represent the transmission power, angular velocity, and translation speed of the three-phase motor. From Equation (1), it can be concluded that there is a linear relationship between the force F and the power P . Therefore, the health status of the switching mechanism can be obtained by analyzing the power curve of the switching mechanism, and the status evaluation of the whole cycle can be carried out.

2.1. Normal power curve of S700K switch machine. The action process of the switch machine mainly includes five stages: start, unlock, transform, lock and express. Figure 1 shows the standard operation power curve of the electric switch machine S700K. In the start and unlock stages, switch start relay is connected, switch indicates circuit is disconnected, the motor is charged, then lock tongue pops up, and complete switch machine unlock. After unlocking, the action bar drives the switch rail to run normally, and the power curve maintains at about 0.5 kW.

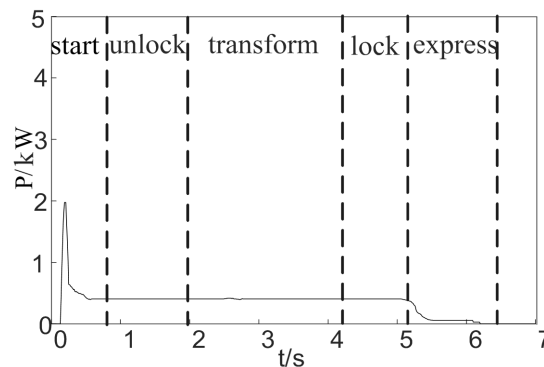


FIGURE 1. Normal power curve of S700K switch machine

Converting stage: the start relay continues to be turned on, the motor drives the rolling screw to rotate counterclockwise, the switch is from positioning to reverse, and the switch conversion is completed when the tip rail moves 220 mm.

Locking stage: the bolt pops out, the connector is locked and held, the three-phase motor is de-energized, and the rotation is stopped.

Expressing stage: when the BHJ falls, the 1DQJ circuit is disconnected, and the reverse position indication circuit is turned on. Because the starting relay has a slow release, the power is reduced to 0 kW after a “small step” occurs.

2.2. S700K switch machine sub-health, fault power curve. According to field investigation results, the operation of the switch machine can be divided into health, sub-health, failure, and severe failure, and the corresponding typical running state power curve is shown in Figure 2. The causes and phenomena corresponding to the curves in Figure 2 are shown below.

d_0 : there is a peak when unlocking, the transition phase is smooth and the transition is maintained at about 0.5 kW, and a small step appears after locking.

d_1 : the loop current is too large, after the switch is in place, the outdoor output voltage is still 380 V during the 1DQJ buffer time, the indoor load for the said circuit rectifier stack, under normal circumstances around two phase current is 0.5 A, curve d_1 slightly

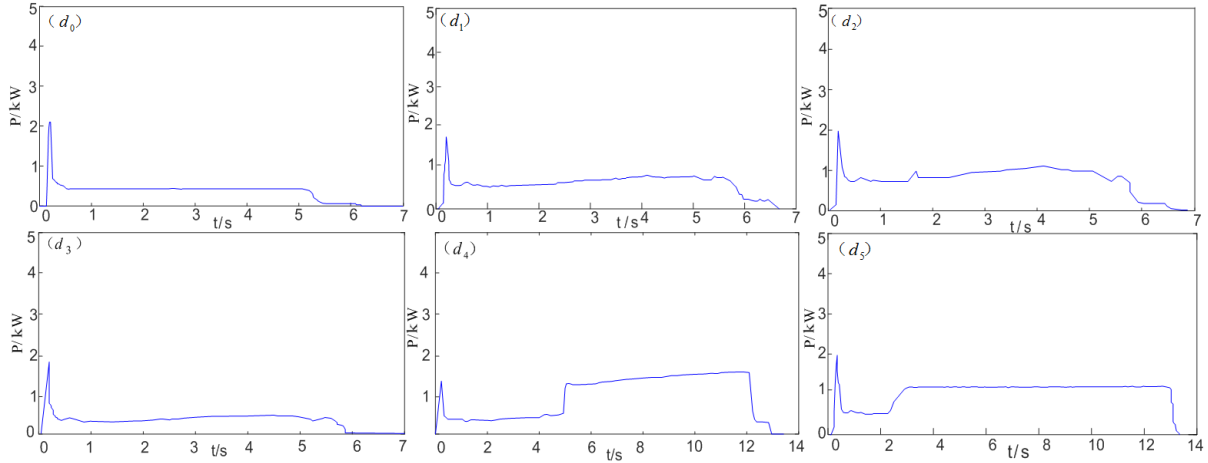


FIGURE 2. Different health status curves

larger than normal power curve of small steps, and like this small steps changes, indicating that the circuit is abnormal, the reason is that the rectifier is bad.

d_2 : the switch installation is not standard. The curve fluctuates in a small range during the switch conversion process, but the switch can be converted into place and locked, indicating that the circuit can be connected normally. The possible reason for this phenomenon is that the installation of a rod of the switch machine is loose or non-standard.

d_3 : the rectifier stack is open, and the switching time of the switch is within the normal range, but the “small step” disappears, and there is no residual current to reflect that the circuit is not connected. The main reason for this phenomenon is that the end of the circuit is faulty.

d_4 : the contact is not driven, the conversion time is too long, indicating that the resistance is large or the conversion force is small. The switch is about 5 s, and the blockage appears in the locking stage, indicating that the blockage appears after the two sharp rails have been basically in place. This phenomenon indicates that the contact is not driven.

d_5 : when the train passes the turnout, the turnout position is incorrect, and the sharp rail fails to close with the basic rail. At this time, the turnout is not in the reverse position, nor in the positioning, showing a four-open state, which is easy to cause the train derailment and overturn.

Six time-frequency domain characteristic statistics of absolute mean, root mean square, standard deviation, variance, peak factor and margin factor in Table 1 were selected to represent the characteristics of the switch machine under different operating states, taking sensitivity and stability into consideration. In Figure 2, the corresponding parameters of Table 1 are extracted from the curve to obtain Table 2, when the switch machine fails, the corresponding time-frequency domain characteristic parameters change greatly, so as to judge the failure of the switch machine, but using the characteristic indexes cannot accurately identify switch machine running state.

3. Constructing Feature Extraction Model Based on Residual Network.

3.1. Convolutional residual networks. Deep learning is mainly through the construction of multi-layer networks, using in-depth features to express data information. In recent years, convolutional neural network (CNN) has made breakthroughs in various fields, especially in image processing and feature extraction [15-18]. More and more scholars have applied CNN in fault diagnosis. After the convolution operation, the convolutional neural

TABLE 1. Time-frequency domain calculation method

Algorithm	Calculation formula
Absolute mean μ_1	$\mu_1 = \frac{1}{n} \sum_{i=1}^n x_i $
Root mean square μ_2	$\mu_2 = \sqrt{\frac{1}{n} \sum_{i=1}^n x_i^2}$
Standard deviation μ_3	$\mu_3 = \sqrt{\frac{1}{n} \sum_{i=1}^n (x_i - \mu_1)^2}$
Variance μ_4	$\mu_4 = \frac{1}{n} \sum_{i=1}^n (x_i - \mu_1)^2$
Crest factor μ_6	$\mu_6 = \frac{\max_{i=1}^n(x_i)}{\sqrt{\frac{1}{n} \sum_{i=1}^n x_i^2}}$
Clearance factor μ_7	$\mu_7 = \frac{\max(x_i)}{\left(\frac{1}{n} \sum_{i=1}^n \sqrt{x_i^2}\right)^2}$

TABLE 2. Characteristic parameters in time and frequency domain

	d_0	d_1	d_2	d_3	d_4	d_5
Absolute mean	0.4028	0.6544	0.8254	0.8146	1.0110	0.9388
Root mean square	0.4577	0.7216	0.8743	0.8683	1.0824	1.0557
Standard deviation	0.2187	0.3036	0.2901	0.3328	0.5438	0.3061
Variance	0.0478	0.0937	0.0842	0.0967	0.2957	0.0937
Crest factor	4.1929	2.4577	2.0238	2.0379	1.4266	1.1024
Clearance factor	5.0797	2.8890	2.2614	2.3128	1.8762	1.2594

network takes the image as input and extracts local features in the pooling layer [19]. Convolution operation can be seen as “filter operation”, and its convolution form is

$$x_j^l = f \left(\sum_{i \in M_j} x_i^{l-1} \cdot k_{ij}^l + b_j^l \right) \tag{2}$$

In the formula, x_j^l is the j -th feature map of l layer; f is the activation function; k_{ij}^l is convolution kernel; M_j is the feature set; b_j^l is the j -th offset of l layer.

After the convolution operation, it enters the pooling layer, reduces the size of the matrix, reduces the parameters of the neural network, and enters the classification layer after the feature vector is formed. The more classical convolutional neural networks in convolutional neural networks mainly include LeNet-5, AlexNet, VGGNet, and ResNet. Compared with other network structures, the residual structure “Shortcut Connection” of ResNet can directly connect and transmit the input data information to the output. The problem of gradient disappearing and accuracy decreasing with the increase of layers is solved. The structure of ResNet-18 is shown in Figure 3.

ResNet-18 has been trained with millions of images and has rich feature representation ability. Figure 3 has four residual blocks, each residual block has two layers, and each layer

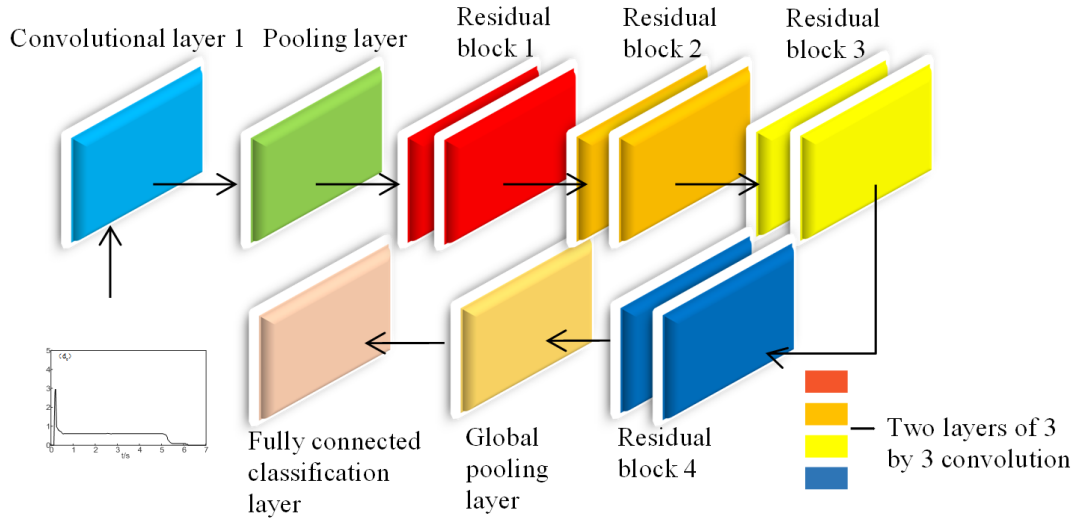


FIGURE 3. ResNet-18 structure

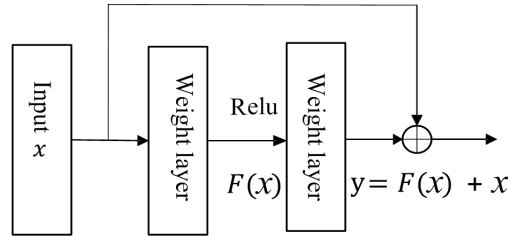


FIGURE 4. Residual block structure

contains two $3 * 3$ convolutional layers. In addition, there are conv1 and full connection classification layers, a total of 18 layers. The structure of the ResNet residual block is shown in Figure 4. The residual structure in the figure has two layers. The residual function is formed by input x through residual learning. In Figure 4, there is the following expression:

$$F = W_2\sigma(W_1x) \tag{3}$$

In the formula, σ is the activation function Relu, and after “Shortcut” and the second layer Relu, W_1 is the first convolution operation, and W_2 is the second convolution operation. The output y is obtained, and y has two output expressions. When the number of channels remains unchanged,

$$y = F(x, \{W_i\}) + x \tag{4}$$

When the output channel changes, as shown in Figure 5, when the number of channels changes from 64 to 128, it is a dashed line connection. At this time, “Shortcut” makes a linear change W_s for x , as shown in the following formula:

$$y = F(x, \{W_i\}) + W_sx \tag{5}$$

In the above formula, x is the input and y is the output of the neural network, which is convolution to adjust the dimension of the channel. It can be seen from the residual network structure that the first 17 layers are the feature extraction layer, and the 18th layer is the classification layer. In this paper, ResNet-18 is used as the model, and the first 17 layers are used as the feature extractor to extract the features of the S700K switching power curve and output its features.

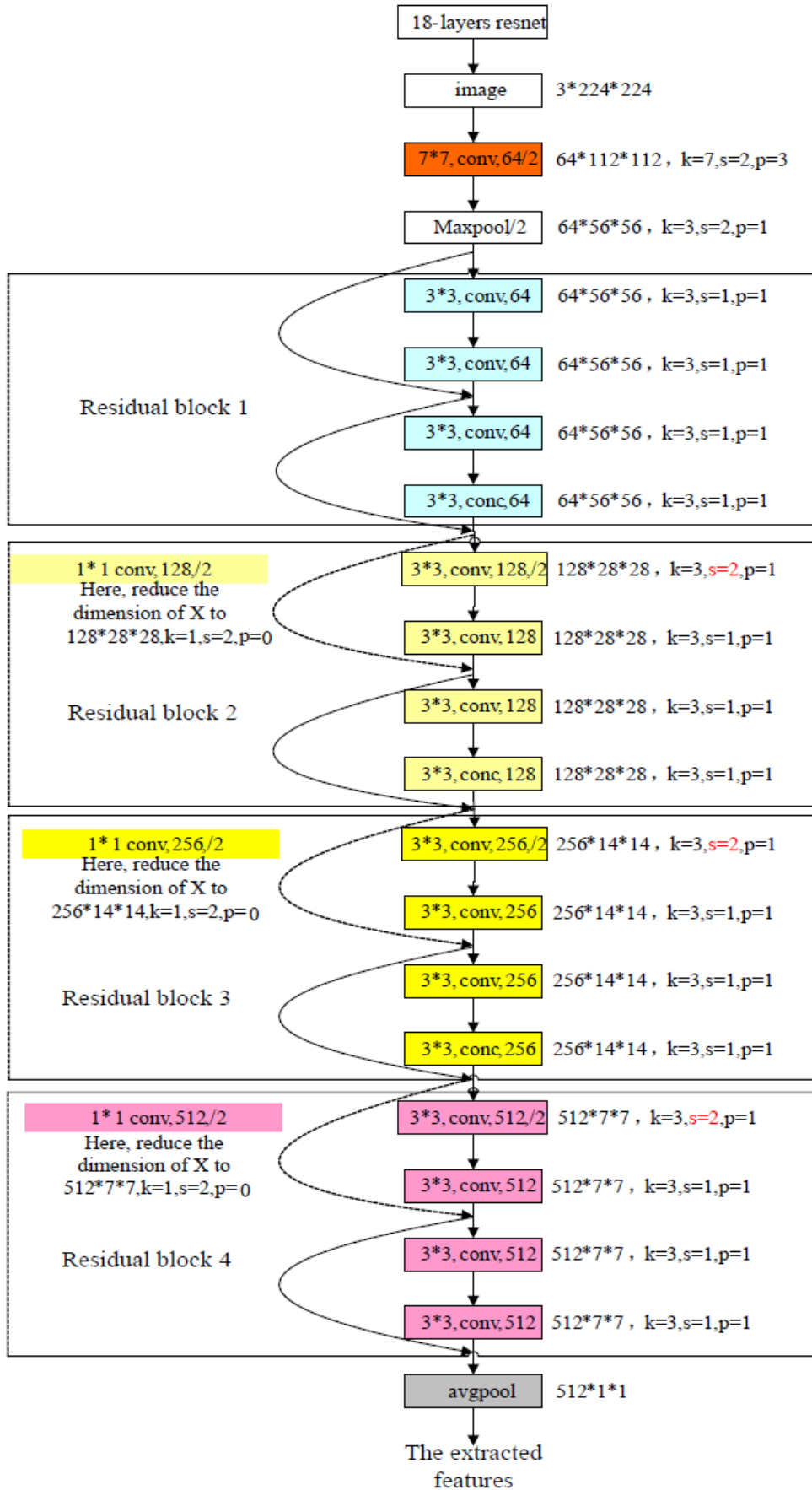


FIGURE 5. Residual network feature extraction process

In Figure 5, the first layer is the convolution layer of $7 * 7$, followed by the pooling layer of $7 * 7$, and then through the residual block stacked in some columns, the information flow in the residual block is divided into two parts: one part is residual function $F(x)$ and the other part is identity mapping. After the sum of the two information flows, the residual block is formed through nonlinear activation. The learning process of the residual network can be expressed as follows:

$$\begin{cases} z^{t+1} = w^{t+2}x^t + b^{t+1} \\ x^{t+1} = hz^{t+1} \\ z^{t+2} = w^{t+2}x^{t+1} + b^{t+2} \\ x^{t+2} = h(z^{t+2} + x^t) \end{cases} \quad (6)$$

where z represents the intermediate output; w represents the weight; b represents the offset quantity; h is the nonlinear activation function. Compared with traditional CNN, the residual network directly copies x^t to the deep layer of the network. In x^{t+2} , the *Relu* activation function directly acts on $z^{t+2} + x^t$, namely the residual block.

3.2. Feature extraction of residual network of S700K power curve. The residual block has two structures, namely $3 * 3$ structure and $1 * 1$, $3 * 3$ structure, which are suitable for external and deep networks, respectively. Since the power curve of the switching maneuver is relatively simple, the $3 * 3$ residual structure is used to construct ResNet-18 to extract feature vectors.

The residual network ResNet-18 was used as a feature extractor, six S700K power curve images of four health states were input into ResNet-18, the feature vectors of the power curve of the switch machine were extracted at the global pooling layer, and the feature vector set was established. The specific process is that the S700K switch machine's power curve image is first input into the structure shown in Figure 5 after dimensional adjustment with Matlab. After going through the convolution layer and pooling layer, the residual module is entered. The features after convolution are combined with the original input after dimensionality reduction. Five hundred and twelve feature vectors of the S700K action power curve image in the global pooling layer (AvgPool) are output by the activation function, as shown in Table 3. The feature vector matrix composed of feature vectors of multiple curves will be used for subsequent state clustering.

TABLE 3. Eigenvector matrix

A healthy state	1	2	3	4	5	...	508	509	510	511	512
d_0	0.56	0.69	0.65	0.96	0.17	...	1.93	0.51	0.72	0.28	1.28
d_1	0.30	0.33	0.54	0.64	0.82	...	1.69	1.00	0.34	0.57	2.00
d_2	1.55	0.89	0.24	1.22	0.01	...	0.65	1.02	0.82	0.52	0.94
d_3	1.56	0.28	0.22	0.73	0.12	...	1.97	0.22	0.84	0.16	0.28
d_4	1.05	0.51	0.19	0.46	0.07	...	0.46	0.63	0.18	0.03	0.72
d_5	1.10	0.68	0.14	0.46	0.13	...	0.51	0.88	0.83	0.19	0.90

4. Analysis of Fuzzy Clustering Algorithm. Fuzzy clustering, as an unsupervised learning method, is different from neural network classification. The most significant advantage of clustering is that it does not need any training data to "learn". Only similar objects can be gathered together by fuzzy operation. Fuzzy clustering introduces the principle of fuzzy mathematics into cluster analysis and introduces the similarity index $r_{ij} = R(x_i, x_j)$. After calibration, the fuzzy equivalent matrix is obtained using the tran-

sitive closure method, and the dynamic clustering graph is obtained when λ changes from 0 to 1. The specific process is as follows.

Step1: Data standardization

The data includes N types, and the domain of the classified object is set as $X = [x_1, x_2, \dots, x_n]$. Each object has a indicators for its behavior, namely $X_i = (x_{i1}, x_{i2}, \dots, x_{ia}), i = 1, 2, \dots, n$. The corresponding data matrix is obtained:

$$x = \begin{bmatrix} x_{11} & x_{12} & \cdots & x_{1a} \\ x_{21} & x_{22} & \cdots & x_{2a} \\ \vdots & \vdots & \ddots & \vdots \\ x_{n1} & x_{n2} & \cdots & x_{na} \end{bmatrix} \tag{7}$$

In order to solve the problem that different data lead to different dimensions and adapt to the requirements of fuzzy clustering on data, translation standard deviation and translation range transformation are usually performed on data x :

$$x'_{ik} = \frac{x_{ik} - \bar{x}_k}{s_k} \tag{8}$$

In the formula, $i = 1, 2, \dots, n; k = 1, 2, \dots, m;$

$$\bar{x}_k = \frac{1}{n} \sum_{i=1}^n x_{ik}; \quad s_k = \sqrt{\frac{1}{n} \sum_{i=1}^n (x_{ik} - \bar{x}_k)^2} \tag{9}$$

The translation standard deviation resolves the dimensionality of the data, but there is something else $x'_{ik} \notin (0, 1)$; therefore, the range transformation x'_{ik} is required:

$$x''_{ik} = \frac{x'_{ik} - \min_{1 \leq i \leq n} \{x'_{ik}\}}{\max_{1 \leq i \leq n} \{x'_{ik}\} - \min_{1 \leq i \leq n} \{x'_{ik}\}} \tag{10}$$

At this point, all $x'_{ik} \in (0, 1)$, eliminate the influence of dimension.

Step2: Establish fuzzy similarity matrix (calibration)

The fuzzy matrix is obtained by Step1. In order to further realize clustering, it is necessary to calculate the similarity degree r_{ij} between samples and establish the fuzzy similarity matrix R , which is also known as calibration. The distance method is the primary method to determine r_{ij} as shown below.

Distance method:

$$r_{ij} = 1 - cd(x_i, x_j) \tag{11}$$

Hamming distance:

$$d(x_i, x_j) = \sum_{k=1}^m |x_{ik} - x_{jk}| \tag{12}$$

Euclidean distance:

$$d(x_i, x_j) = \sqrt{\sum_{k=1}^m (x_{ik} - x_{jk})^2} \tag{13}$$

In this paper, Euclidean distance method is used to determine r_{ij} .

Step3: Establish the fuzzy equivalent matrix

According to the above Step2 calibration, the matrix may not be transitive, and R needs to be transformed into an equivalent matrix R^* for classification. That is, starting from R , find the quadratic in turn $R \rightarrow R^2 \rightarrow R^4 \rightarrow \dots \rightarrow R^{2^i} \rightarrow \dots$. After a finite number of operations, it is $R^k \circ R^k = R^k$. In this case, R^k is transitive, and R^k is the equivalent matrix R^* .

Step4: Cluster analysis

After the above steps, the fuzzy equivalent matrix R^* is obtained, for different λ . For any $\lambda \in [0, 1]$, call $R_\lambda = (r_{ij}(\lambda))$. We call $R_\lambda = (r_{ij}(\lambda))$ the λ -intercept matrix of the fuzzy equivalent matrix R^* . Among them,

$$r_{ij}(\lambda) = \begin{cases} 1 & r_{ij} \geq \lambda \\ 0 & r_{ij} < \lambda \end{cases} \quad (14)$$

When $R_{ij} \geq \lambda$ exists, the two samples are grouped together. For different confidence levels $\lambda \in [0, 1]$, different clustering results can be obtained to form a dynamic clustering graph.

The fuzzy clustering of unsupervised classification method is used to replace the softmax classification layer of residual network, and the feature vector matrix is constructed according to the switch machine features output by the global mean pooling layer. The fuzzy equivalent matrix of the matrix is obtained by the fuzzy clustering analysis algorithm. In the fuzzy equivalent matrix, when λ (variable threshold) changes at $[0, 1]$, the fuzzy equivalent matrix is transformed into the equivalent Boolean matrix, and the dynamic clustering graph and classification result can be obtained from the Boolean matrix, so as to realize the state evaluation of switch machine.

5. Method Validation and Analysis.

5.1. Evaluation process. S700K point machine state evaluation process is shown in Figure 6.

Step1: Input the S700K switch machine state library curve and the curve image to be tested into ResNet-18, extract features through the convolution layer and four residual blocks, and extract 512 features in the global pooling layer avgpool.

Step2: Establish feature vector matrix of extracted features, obtain fuzzy similarity matrix by using fuzzy clustering algorithm, and form dynamic clustering graph to obtain diagnosis results.

5.2. Data verification. In order to verify the feasibility of this method, fault power curves of the S700K point machine in two different periods at a site of Lanzhou Bureau were collected, as shown in Figure 7, in which curves f_1, f_2, f_3 were to be tested respectively. The three operating states are found to be consistent with d_5, d_0 and d_2 after on-site

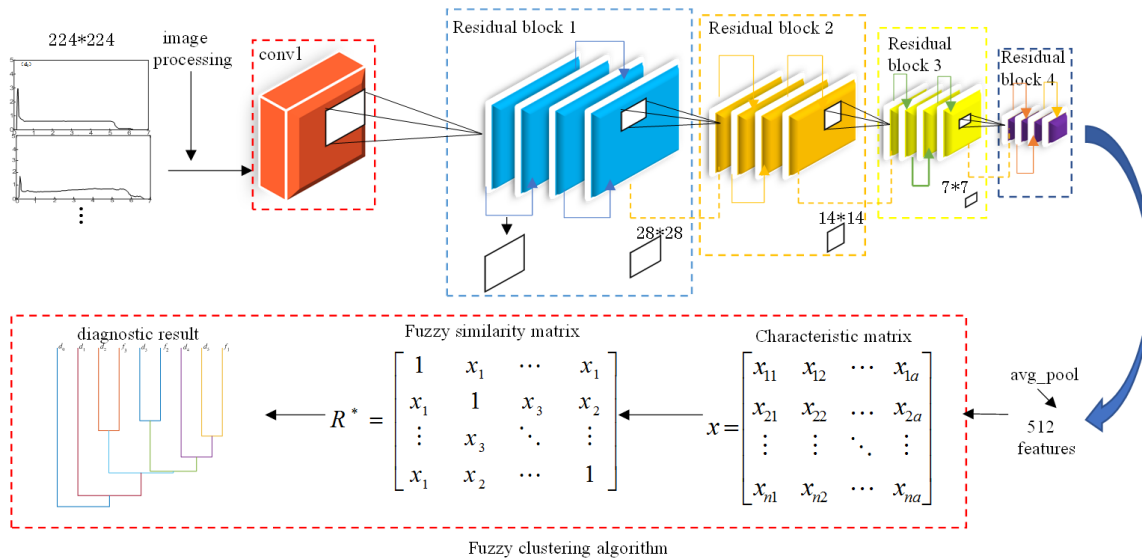


FIGURE 6. S700K switch machine status diagnosis process

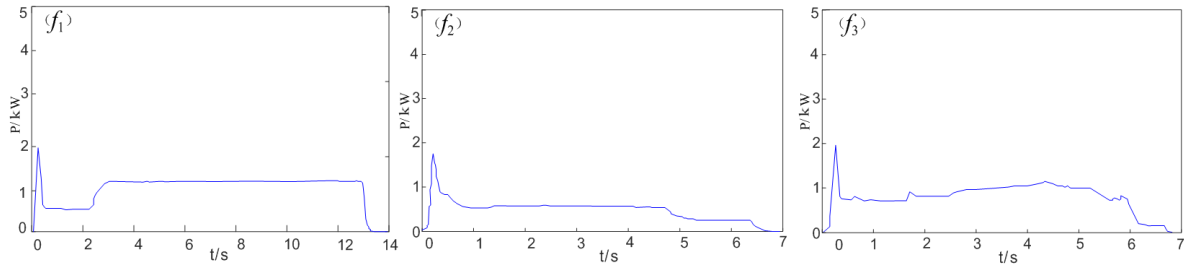


FIGURE 7. Curve to be inspected

TABLE 4. Feature vectors of curves to be tested

Curve to be inspected	1	2	3	4	5	...	508	509	510	511	512
f_1	1.10	0.26	0.08	0.56	0.18	...	0.65	0.74	0.50	0.03	0.93
f_2	0.13	0.98	0.51	0.63	0.31	...	1.82	0.95	0.48	0.29	0.15
f_3	1.19	0.44	0.74	0.89	0.33	...	0.36	0.93	0.13	0.10	1.66

inspection and maintenance. Residual network ResNet-18 was used to extract features of the fault power curve, as shown in Table 4.

According to Table 2 and Table 3, the eigenvector matrix is established. According to the steps of the fuzzy clustering algorithm in Section 4, the feature vector matrix data is standardized so that the data is distributed between 0 and 1, and matrix X is obtained.

$$X = \begin{bmatrix} 0.4934 & 0.0745 & 0.2985 & \dots & 0.3831 & 0.5350 & 0.6192 & 0.1589 \\ 0.1293 & 0.0964 & 0.7595 & \dots & 1 & 1 & 0.4869 & 1 \\ 0.0835 & 0.4157 & 1 & \dots & 0.1583 & 0.2195 & 0.7122 & 0.8924 \\ 0.3662 & 0.4705 & 0.3556 & \dots & 0 & 0.9064 & 0.4231 & 0.0618 \\ 1 & 0.9780 & 0.6105 & \dots & 0.4183 & 0.1639 & 0.1117 & 0.2866 \\ 0.7041 & 0 & 0 & \dots & 0.6108 & 0.8195 & 0 & 0.2152 \\ 0.7394 & 0.1444 & 0.1957 & \dots & 0.9812 & 0.7616 & 0.0347 & 0.3735 \\ 0 & 1 & 0.7648 & \dots & 0.5695 & 0.9931 & 0.5162 & 0 \\ 0.7923 & 0.4431 & 0.8596 & \dots & 0.5141 & 0 & 1 & 0.6068 \end{bmatrix}$$

The above matrix has 9 rows and 512 columns, respectively d_0 to f_3 . In order to determine the sample similarity degree r_{ij} , the fuzzy equivalent matrix R is obtained by using the Euclidean distance method to calibrate matrix X . The matrix R is transformed into fuzzy similarity matrix R^* by the Step3 method:

$$R^* = \begin{bmatrix} 1 & 0.1880 & 0.1880 & 0.3371 & 0.2402 & 0.2402 & 0.2402 & 0.5221 & 0.1880 \\ 0.1880 & 1 & 0.4081 & 0.1880 & 0.1880 & 0.1880 & 0.1880 & 0.1880 & 0.4081 \\ 0.1880 & 0.4081 & 1 & 0.1880 & 0.1880 & 0.1880 & 0.1880 & 0.1880 & 0.6952 \\ 0.3371 & 0.1880 & 0.1880 & 1 & 0.2402 & 0.2402 & 0.2402 & 0.3371 & 0.1880 \\ 0.2402 & 0.1880 & 0.1880 & 0.2402 & 1 & 0.3019 & 0.3019 & 0.2402 & 0.1880 \\ 0.2402 & 0.1880 & 0.1880 & 0.2402 & 0.3019 & 1 & 0.7016 & 0.2402 & 0.1880 \\ 0.2402 & 0.1880 & 0.1880 & 0.2402 & 0.3019 & 0.7016 & 1 & 0.2402 & 0.1880 \\ 0.5221 & 0.1880 & 0.1880 & 0.3371 & 0.2402 & 0.2402 & 0.2402 & 1 & 0.1880 \\ 0.1880 & 0.4081 & 0.6952 & 0.1880 & 0.1880 & 0.1880 & 0.1880 & 0.1880 & 1 \end{bmatrix}$$

In the fuzzy similarity matrix R^* , when the confidence factor λ changes from small to large, a dynamic clustering graph is formed, as shown in Figure 8. When $\lambda = 0.702$, curve f_1 and curve d_5 to be detected are similar to each other and classified as one class. When $\lambda = 0.522$, the curve f_2 to be measured is consistent with curve d_0 and is classified as

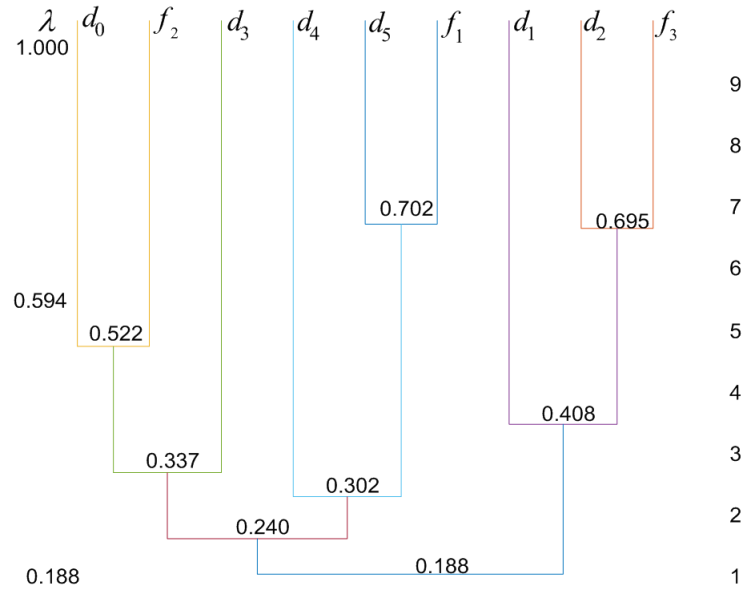


FIGURE 8. Cluster diagram of fault detection results

TABLE 5. Comparison of the accuracy of the five algorithms

Algorithm	Fault library samples/each	Test samples/each	Diagnostic accuracy
SVM	6	36	88.89%
BP	6	36	83.33%
KNN	6	36	91.67%
1D-CNN	—	36	77.78%
Diagnostic accuracy	6	36	97.22%

normal. When $\lambda = 0.695$, the installation of f_3 and d_2 sub-healthy switch is not similar to standard and is classified as one class. This is consistent with the field test result.

In order to compare the superiority of the proposed algorithm with the current mainstream time-frequency domain and 1D-CNN fault diagnosis algorithm, the features extracted in Table 2 are input into SVM, BP, KNN and 1D-CNN for comparison, and 36 groups of data are collected from microcomputer monitoring for verification. The diagnostic accuracy is shown in Table 5. It can be seen from the table that the algorithm in this paper has high classification accuracy in the case of small samples.

6. Conclusion. In this paper, the combination of image feature extraction and fuzzy clustering in deep learning is applied to the state diagnosis of the point machine. The first 17 layers of ResNet-18 were used as the feature extractor, and the S700K action power graph was input into the feature extractor. After multi-layer convolution and residual operation, features were extracted in the global pooling layer of ResNet-18. Due to the powerful feature extraction capability, the ResNet-18 model, the micro-state characteristics of the S700K switch power curve are extracted.

The extracted features are built into a feature vector matrix, and the fuzzy clustering analysis algorithm is used for classification, and the dynamic clustering results are obtained according to different confidence factors. When the confidence factor takes a specific value, the highest similarity is classified into one category to achieve the S700K, the purpose of evaluating the functional status of the switch machine.

This method utilizes the feature extraction capability of the convolutional residual network for images and the unsupervised learning method of fuzzy clustering. It has the advantages of self-adaptation and small sample size and can realize the full-cycle state assessment of the S700K switch machine without data training.

REFERENCES

- [1] Z. Zhong, T. Tang and F. Wang, Research on fault feature extraction and diagnosis of railway switches based on PLSA and SVM, *Journal of the China Railway Society*, vol.40, no.7, pp.80-87, 2018.
- [2] W. Wei and X. Liu, Fault diagnosis of S700K switch machine based on EEMD multiscale sample entropy, *Journal of Central South University (Science and Technology)*, vol.50, no.11, pp.2763-2772, 2019.
- [3] R. Wang and W. Chen, Research on fault diagnosis method of S700K switch machine based on grey neural network, *Journal of the China Railway Society*, vol.38, no.6, pp.68-72, 2016.
- [4] Y. Chi and W. Chen, Real-time turnout fault diagnosis based on one-dimensional convolutional neural network, *Computer Engineering and Applications*, pp.1-9, 2021.
- [5] W. Hu and S. Qiu, Ultrasonic detection and classification for internal defect of rail based on deep learning, *Journal of the China Railway Society*, vol.43, no.4, pp.108-116, 2021.
- [6] C. Shi, Movable/static contact state detection technology of metro turnout switch machine based on image processing, *Research on Urban Rail Transit*, vol.23, no.S2, pp.149-152, 2020.
- [7] B. Luo, H. Wang, H. Liu et al., Early Fault Detection of Machine Tools Based on Deep Learning and Dynamic Identification, *IEEE Transactions on Industrial Electronics*, vol.66, no.1, pp.509-518, 2019.
- [8] Y. Wu, M. Huang, Y. Li, S. Feng and W. Di, A distributed fusion framework of multispectral and panchromatic images based on residual network, *Remote Sensing*, vol.13, no.13, pp.177-180, 2021.
- [9] B. Hou, X. Yang, L. Gao, H. Xiao and S. Ma, Identification of track structure disease based on deep residual network, *Journal of the China Railway Society*, vol.42, no.8, pp.100-106, 2020.
- [10] Z. Liu, H. Chen and Z. Ren, Deep learning audio magnetotellurics inversion using residual-based deep convolution neural network, *Journal of Applied Geophysics*, vol.188, 104309, 2021.
- [11] F. Deng, H. Ding, S. Yang and R. Hao, An improved deep residual network with multiscale feature fusion for rotating machinery fault diagnosis, *Measurement Science and Technology*, vol.32, no.2, 2021.
- [12] Q. Xue and X. Huang, Evaluation of the suitability of human settlement environment in Shanghai city based on fuzzy cluster analysis, *Thermal Science Journal*, vol.24, no.4, pp.2543-2551, 2020.
- [13] D. Wei, X. Liu and Z. Shan, Fuzzy cluster analysis of weapon system of systems based on entropy weight and grey relational degree, *Journal of Information Engineering University*, vol.21, no.5, pp.626-630, 2020.
- [14] M. Medhat, Y. F. Hassan and A. Elsayed, Humans and bots web session identification using K-means clustering, *ICIC Express Letters*, vol.13, no.12, pp.1149-1156, 2019.
- [15] P. Zhang, F. Li, R. Zhao and L. Du, Real-time psychological stress detection according to ECG using deep learning, *Applied Sciences*, vol.11, no.9, p.3838, 2021.
- [16] T. Ince, S. Kiranyaz, L. Eren, M. Askar and M. Gabbouj, Real-time motor fault detection by 1-D convolutional neural networks, *IEEE Transactions on Industrial Electronics*, vol.63, no.11, pp.7067-7075, 2016.
- [17] O. V. Ilina and M. V. Tereshonok, Robustness study of a deep convolutional neural network for vehicle detection in aerial imagery, *Journal of Communications Technology and Electronics*, vol.67, no.2, pp.164-170, 2022.
- [18] A. Hannun, P. Rajpurkar and M. Haghpanahi, Cardiologist-level arrhythmia detection and classification in ambulatory electrocardiograms using a deep neural network, *Nature Medicine*, vol.25, no.1, pp.65-69, 2019.
- [19] Y. Lecun, K. Kavukcuoglu and C. Farabet, Convolutional networks and applications in vision, *Proc. of 2010 IEEE International Symposium on Circuits and Systems*, pp.253-256, 2010.

Author Biography



Wenjun Wei is a doctor of engineering, a professor and a graduate tutor. He is a critical member of the innovation team of “Changjiang Scholars and Innovation Team Development Plan” of the Ministry of Education, “Research on a Complete Set of Coating Equipment and Coating Process of Computer Fully Automatic Control of Ultra-Large Volume Automobile Lamps and Lanterns” of the national key problem-solving plan, and “Research, Development, and Transformation of Railway Station Full Electronic Intelligent Control Series Module” of the national innovation fund. He presided over 2 provincial and ministerial scientific research projects, participated in 7 provincial projects, and obtained 4 invention patents and 3 utility model patents as a major member. He has published more than 20 academic papers, which have been indexed by EI, ISTP, and many domestic core journals. Research interests include multi-agent cooperative control and optimization, fault diagnosis of dynamic systems, and intelligent control theory and application.



Xuanming Zhang is a postgraduate student in the School of Automation and Electrical Engineering, Lanzhou Jiaotong University, Gansu, China. His research interests include fault diagnosis and life prediction of switch machines and bearings.



Liben Yang received the B.Eng. degree in communication engineering from Kunming University of Science and Technology, China, 2000; the M.Sc. degree in communication and information system from Kunming University of Science and Technology, China, 2009; the Ph.D. degree in control science and Engineering, from Northwest University of Technology, China, 2017.

Dr. Yang is currently a full-time associate professor at the College of Automation and Electrical Engineering, Lanzhou Jiaotong University, China. His main research interests include UAV control system, UAV autonomous intelligent control and intelligent control system based on reinforcement learning. He has published more than ten papers in well-known journals.